Curvature and Zeeman effects on persistent currents in a multi-walled carbon nanotorus*

Xu Ning(徐 宁), Ding Jian-Wen(丁建文)†, Ma Ming-Ming(马明明), and Tang Xian(汤 贤)

Department of Physics and Institute for Nanophysics and Rare-earth Luminescence, Xiangtan University, Xiangtan 411105*, China*

(Received 23 April 2009; revised manuscript received 23 June 2009)

Taking into account both the intrinsic curvature and Zeeman effects, persistent currents in a multi-walled carbon nanotorus are explored by using a supercell method, within the tight-binding formalism. It is shown that in the absence of the Zeeman effect, the intrinsic curvature induces some dramatic changes in energy spectra and thus changes in the shape of the flux-dependent current. A paramagnetism–diamagnetism transition is observed. With consideration of the Zeeman splitting energy, the period of persistent current is destroyed, and a diamagnetism–paramagnetism transition is obtained at high magnetic field. In addition, we further explore the effect of external electric field energy ($E_{\rm ef}$) on persistent current, indicating that it changes unmonotonously with $E_{\rm ef}$.

Keywords: multi-walled carbon nanotorus, tight-binding model, persistent current
PACC: 6148, 1340F, 7115F

1. Introduction

The discovery of toroidal carbon nanotubes (TCNs), which can be considered to be constructed by bending a carbon nanotube (CNT), has attracted much attention in recent years[1−29]. Because of the novel honeycomb ring structure, TCNs appear to be ideal candidates for one to explore the magnetic response mechanism of microscopic rings. Some works have been reported on this subject. Of special interest is the persistent current ($I_{\rm pc}$) and magnetic response in such a thin ring-shaped topology, which has been addressed in several corresponding works.[11−14,18−20]

Recently, a multi-walled carbon nanotorus (MWTCN) has been synthesized experimentally.[26,27] Theoretically, it can be formed by joining the two ends of a conventional multi-walled carbon nanotube (MWCNT). Based on the CNT model, Chen *et al.*[30] calculated the persistent current in MWTCNs with the outer-wall disorder. It was found that in the regime of weak disorder, the persistent current decreases with disorder strength, while it increases in the regime of strong disorder. Here, the curvatures along the longitude direction were neglected. In a finite sized MWTCN, the curvatures are much more complicated. Similar to the TCN, the local bond characteristic of the torus inner-side differs from that of the torus outer-side,[31] which may lead to more complicated misorientation and rehybridization of the orbitals due to high curvature. Therefore, one can expect that the curvature effects have a pronounced effect on the electronic structure of MWTCNs, and thus the persistent current.

Considering the Zeeman effect, we have investigated the persistent currents of TCN theoretically. It is shown that the Zeeman effect has an important role in determining persistent current. For example, Lin *et al.*[11,17] calculated the persistent currents in TCNs in the presence of Zeeman splitting. It was shown that at low magnetic field, most armchair TCNs are diamagnetic while chiral TCNs are either paramagnetic or diamagnetic. Zeeman splitting leads to the destruction of periodicity at high magnetic field. Similar to the results of TCN, one can expect that Zeeman effects play an important role in determining the persistent current of MWTCNs.

Experimentally, the temperature effect on persistent current should be considered. At nonzero temperature, thermal excitations, such as phonons, are present. Such excitations interact with the inelastically scattered electrons, giving rise to phase random-

*Project supported by the National Natural Science Foundation of China (Grant No. 10674113), Program for New Century Excellent Talents in University of China (Grant No. NCET-06-0707), Foundation for the Author of National Excellent Doctoral Dissertation of China (Grant No. 200726), Scientific Research Fund of Hunan Provincial Education Department of China (Grant No. 06A071), and partially by Hunan Provincial Innovation Foundation For Postgraduate (Grant No. S2008yjscx06).
†Corresponding author. E-mail: jwding@xtu.edu.cn
© 2010 Chinese Physical Society and IOP Publishing Ltd

ization of the electron wavefunction. In this study, we assume that the phase-coherence length (L_ϕ) of the electron is large compared to the MWTCN circumference (L), $L_\phi > L$. It is shown that at low temperature (T), the persistent current decreases slightly with increasing T, while it damps exponentially at high T.

The effects of electric and magnetic fields on the electronic structure of TCNs have been studied with the tight-binding model.[8,32] Metal–insulator transitions were observed. Therefore, one expects that the persistent current ($I_{\rm pc}$) of MWTCNs can be modulated by electric field. In this study, we explore the external field energy ($E_{\rm ef}$) effect on $I_{\rm pc}$ by applying the electric field (E) perpendicularly to the torus plane, as shown in Fig. 1. It is shown that with increasing $E_{\rm ef}$, a paramagnetism–diamagnetism transition is observed. In addition, the typical current ($I_{\rm ty}$) exhibits an oscillation feature with $E_{\rm ef}$, which originates from the energy spectral changes induced by $E_{\rm ef}$. We believe that a much better understanding of the physical properties of MWTCNs, even within such a simple picture adopted here, should help us to suggest their utilization in real nanodevices.

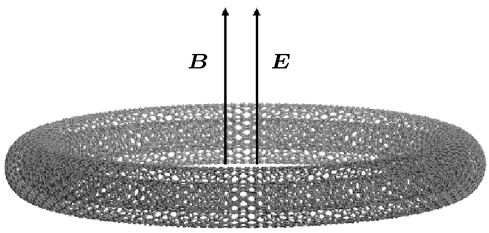


Fig. 1. Schematic of a DWTCN (the applied magnetic field and electric field are perpendicular to the torus plane).

2. Model and method

MWTCNs can be classified into two general categories. One is formed from a commensurate MWCNT. Similar to TCN, its rotational symmetry still remains in this case. The other is formed from an incommensurate MWCNT, in which the rotational symmetry is destroyed. For simplicity, we restrict our analysis only to the commensurate double-walled carbon nanotorus (DWTCN), which is formed from a commensurate (n_1, m_1)@(n_2, m_2) double-walled carbon nanotube with p unit cells, indexed by (n_1, m_1)@(n_2, m_2) $\times$ p.

The DWTCN sample is described by a tight-binding model with one π orbital per atom. With the curvature effect, the three nearest-neighbour intra-torus hopping integrals γ_i (i = 1, 2, 3) are given by $\gamma_i = \gamma_0 f(r_{ij})$ with γ_0 the in-plane hopping integral in the graphite,[33] where the modified factor $f(r_{ij})$ depends on the distance r_{ij} between two nearest-neighbour π-like electronic orbits on the curved surface of a torus. Like the interlayer coupling of the MWCNT, the inter-torus coupling is introduced by

$$\gamma = \frac{\gamma_0}{8}\cos(\theta_{ij})\exp\left(\frac{a-d_{ij}}{\delta}\right) \tag{1}$$

with $\alpha = 0.334$ nm, and $\delta = 0.045$ nm,[33] where θ_{ij} and d_{ij} are respectively the alignment angles and the distance of two π-like electronic orbits between two TCNs. In our model, the cut distance between two TCNs is taken to be 0.4 nm.

In the present paper, we divide averagely the p unit cells into K supercells. In terms of the rotational symmetry, the effective Hamiltonian of a supercell is given by[10,15,34,35]

$$\boldsymbol{H}_{\rm eff} = \boldsymbol{H}_0 + {\rm e}^{{\rm i}\,\beta}\boldsymbol{H}_1 + {\rm e}^{-{\rm i}\,\beta}\boldsymbol{H}_1^+, \tag{2}$$

where $\boldsymbol{H}_0$ and $\boldsymbol{H}_1$ refer to the Hamiltonian matrix in the supercell and the coupling matrix between the two neighbouring supercells, respectively. Here $\beta = j \times 2\pi/K$, (j = 1, 2, 3... , K) is the phase difference between the wave functions of two neighbouring supercells, with K being the number of supercells contained in the system. For a given β, the eigenlevels $E(\phi)$ can be obtained by diagonalizing the matrix $\boldsymbol{H}_{\rm eff}$.

Considering the Zeeman effect, we can write the splitting energy as $\varepsilon_\sigma(\phi) = g\sigma\phi/m_{\rm e}R^2\phi_0$, in which $g = 2$ is the Landau factor, $\sigma = \pm 1/2$ is the electron spin, and $m_{\rm e}$ is the bare electron mass. Therefore, the eigenvalue can be given by

$$E(\sigma,\phi) = E(\phi) + \varepsilon_\sigma(\phi). \tag{3}$$

When we neglect the interaction of electrons and the self-inductance effect, at zero temperature, the total current of a DWTCN can be calculated by the following expression:[13,34,35]

$$I_{\rm pc} = -\sum_n \partial E_n/\partial\Phi = -\frac{1}{\Phi_0}\sum_n \frac{\partial E_n}{\partial\phi}, \tag{4}$$

with the summation running up to the last occupied energy levels.

At a finite temperature T, the electrons occupy higher levels and all the states participate formally to the total free energy. The total current of a DWTCN

can be calculated by

$$I_{\rm pc} = -\sum_n \partial f_n/\partial \Phi = -\sum_n \frac{\partial\left(-k_{\rm B}T\ln\left[1+\exp\left(\frac{E_{\rm F}-E_n}{k_{\rm B}T}\right)\right]\right)}{\partial\Phi}, \quad (5)$$

where $E_{\rm F}$ is the Fermi energy and $k_{\rm B}$ the Boltzmann constant. Usually, one is interested in the typical current, which is defined as the square root of the flux average of the square of the persistent current.[13,34]

$$I_{\rm typ} = \sqrt{\langle I^2\rangle_\Phi}. \quad (6)$$

3. Calculations and discussion

In Fig. 2, (18, 0)@(9, 0)×86 and (10, 10)@(5, 5)×150 DWTCNs are chosen to study the effects of intrinsic curvature and inter-wall interaction on persistent current. Both of the DWTCN samples have almost the same torus-radius. In the absence of both the inter-wall interaction and intrinsic curvature ($\gamma = 0$, $f(r_{ij}) = 1$), it can be seen from Fig. 2 that $I_{\rm pc}$s in the two DWTCNs are merely the superposition of $I_{\rm pc}$s of the constituent inner and outer tori. In the presence of only curvature ($\gamma = 0$, $f(r_{ij}) \neq 1$), the currents are suppressed at small ϕ in both samples, largely lower than that in the absence of curvature ($\gamma = 0$, $f(r_{ij}) = 1$). Additionally, the sawtooth-shape of $I_{\rm pc}$ for the (18, 0)@(9, 0)×86 DWTCN is smoothed due to level anticrossings, which is in contrast with the curve of $I_{\rm pc}$ for the (10, 10)@(5, 5)×150 DWTCN. The smoothed persistent current as a function of flux, owing to level anticrossing, has also been found in TCN.[36] In Fig. 2(b), it is shown that in the presence of only curvature ($\gamma = 0$, $f(r_{ij}) \neq 1$), some new jumps are observed in the (10, 10)@(5, 5)×150 DWTCN, similar to that in the TCN bundles.[13] In the presence of both the inter-wall interaction and intrinsic curvature ($\gamma \neq 0$, $f(r_{ij}) \neq 1$), the amplitudes of $I_{\rm pc}$ for (18, 0)@(9, 0)×86 and (10, 10)@(5, 5)×150 DWTCNs are obtained to be 0.22 eV/Φ_0 and 0.28 eV/Φ_0, respectively. Especially, the magnetism changes from paramagetism to diamagnetism. Therefore, the intrinsic curvature and inter-wall interaction have strong effects not only on the amplitude of $I_{\rm pc}$ but also the magnetic response, both of which should be considered in theoretical simulation.

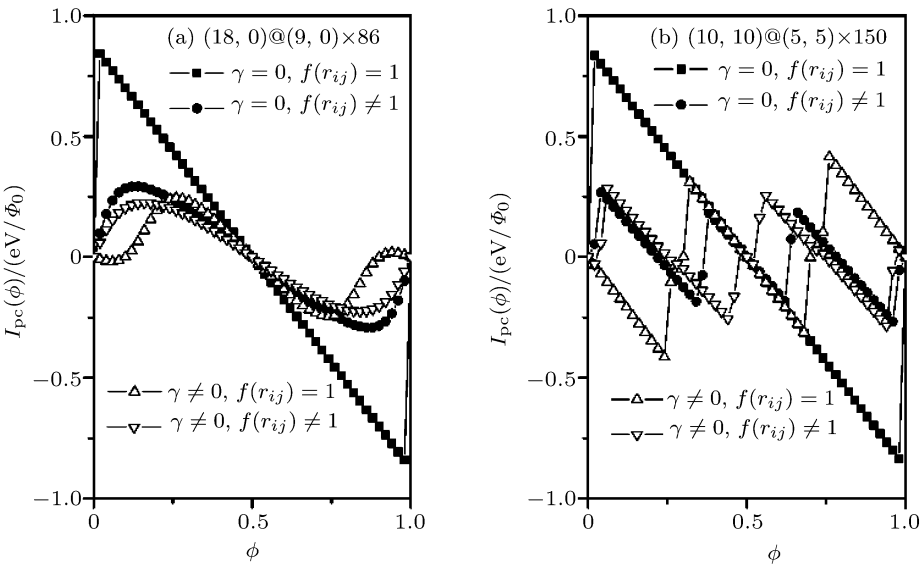


Fig. 2. The persistent current as a function of magnetic flux in (a) (18, 0)@(9, 0)×86 DWTCN and (b) (10, 10)@(5, 5)×150 DWTCN.

By considering the Zeeman effect, in Fig. 3 we show the persistent current as a function of magnetic flux at (a) low and (b) high magnetic fields. It is shown that at low magnetic field, the Zeeman effect has little effect on the persistent current. At high magnetic field, the Zeeman effect strongly affects the low-energy electronic states, and thus the persistent current. Similar to the results for the TCN,[11] the period of persistent current is destroyed. The persistent currents of (18, 0)@(9, 0)×86 and (10, 10)@(5, 5)×150 DWTCNs exhibit some new

jumps due to level crossing. Especially, the magnetism drastically changes from diamagnetism to paramagnetism for some given flux values. Therefore, Zeeman effects cannot be neglected, especially at high magnetic field.

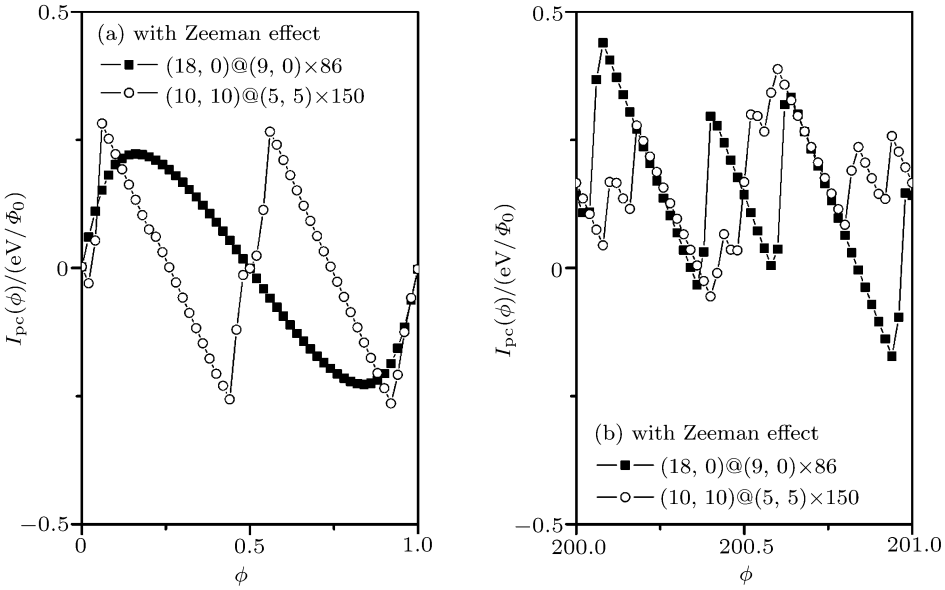


Fig. 3. The magnetic-flux-dependent persistent current in (18, 0)@(9, 0)×86 and (10, 10)@(5, 5)×150 DWTCN at (a) $0 \leq \phi \leq \phi_0$, (b) $200\phi_0 \leq \phi \leq 201\phi_0$.

To explore the effect of temperature, in Fig. 4 we show the typical current versus temperature in the presence of both intrinsic curvature and inter-wall interaction. Here, we assume that the phase coherence length L_ϕ is much larger than L, so that the system remains possible to be fully described by the eigenfunctions of its Hamiltonian. The effect of temperature is to make a distribution of the occupancy around E_F, within k_BT. The characteristic temperature T^* is determined by $T^* = \Delta/2\pi^2 k_B$, where Δ is the level spacing at E_F.[13,30] In this study, the characteristic temperature T^* is about 50 K. It can be seen from Fig. 4 that at $T > T^*$, I_{ty} damps exponentially with increasing T, while it decreases slightly at $T < T^*$. However, T does not destroy the periodicity of AB oscillation, as shown in Fig. 4(b). The decrease of persistent current with T is mainly due to the cancellations between the states below and above E_F. The cancellations are significantly increased with T, and thus an exponentially decaying current can be obtained.

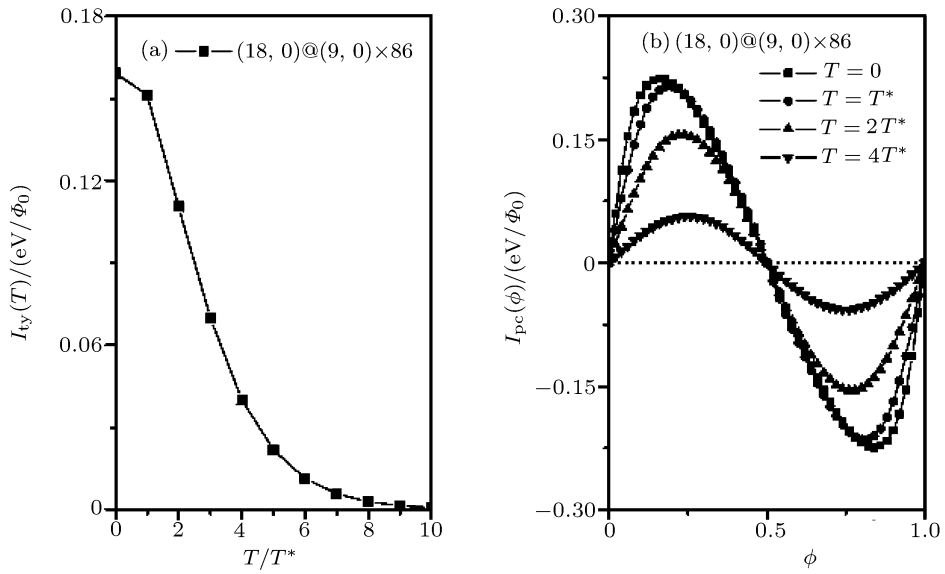


Fig. 4. (a) The typical currents in (18, 0)@(9, 0)×86 DWTCN versus temperature T and (b) the persistent currents in (18, 0)@(9, 0)×86 DWTCN versus magnetic flux at various temperatures.

The external electric field can alter many aspects of energy spectra[8,32] and thus the persistent currents.[31] Figure 5(a) illustrates $I_{\rm ty}$ as a function of $E_{\rm ef}$. It is shown that for the (18, 0)@(9, 0)×86 DWTCN, $I_{\rm ty}$ varies unmonotonously with $E_{\rm ef}$. At higher $E_{\rm ef}(E_{\rm ef} > 1.5\gamma_0)$, $I_{\rm ty}$ exhibits oscillatory feature with a series of isolated sharp peaks. At lower $E_{\rm ef}(E_{\rm ef} < 0.8\gamma_0)$, $I_{\rm ty}$ decreases smoothly. The results show that the electric field energy $E_{\rm ef}$ has significant effects on $I_{\rm ty}$s. To further explore the effect of $E_{\rm ef}$ on persistent current, in Fig. 5(b) we show the persistent current versus flux at various $E_{\rm ef}$. It is shown that the effect of electric field does not destroy the periodicity of AB oscillation, which remains as Φ_0. For $E_{\rm ef} = 0, 1.83\gamma_0$, the (18, 0)@(9, 0)×86 DWCNT exhibits paramagnetism at small ϕ, in which the amplitudes of $I_{\rm pc}$ are obtained to be 0.22 eV/Φ_0, and 0.11 eV/Φ_0. For $E_{\rm ef} = 2\gamma_0$, however, the (18, 0)@(9, 0)×86 DWTCN exhibits diamagnetism at small ϕ, in which the amplitude of $I_{\rm pc}$ is obtained to be 0.01 eV/Φ_0. Variations in $I_{\rm pc}$ arise from the changes of energy spectra induced by $E_{\rm ef}$. Therefore, the persistent current of a DWTCN can be modulated by the external electric field, which is helpful for the design and performance improvement of DWTCN molecular devices.

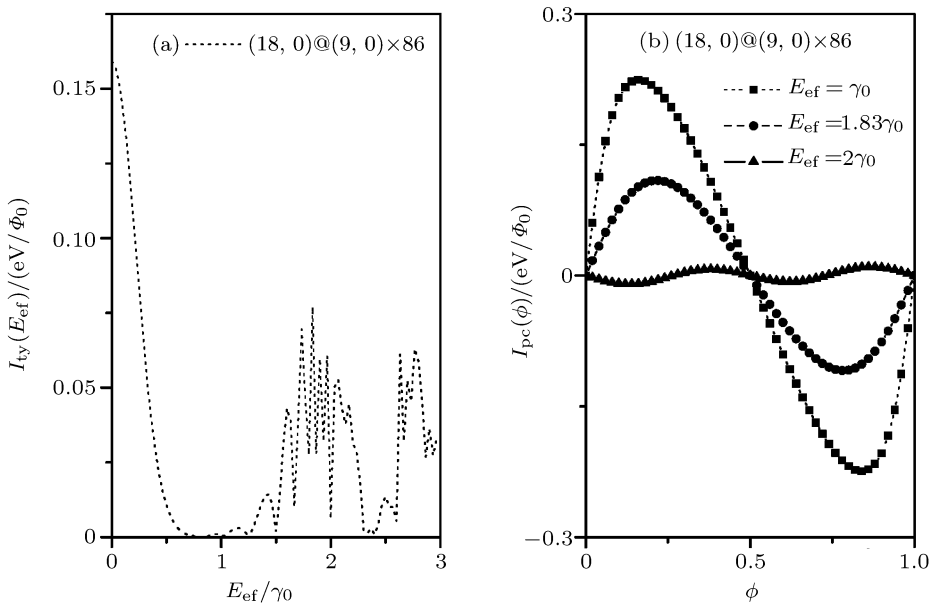


Fig. 5. (a) The dependence of the typical currents on the electric field energies for (18, 0)@(9, 0)×86 DWTCN. (b) The persistent currents versus flux for (18, 0)@(9, 0)×86 DWTCN at various electric field energies.

4. Conclusion

By using the supercell approach, we have calculated the persistent current of an MWTCN in the presence of intrinsic curvature and inter-wall interaction. Studies show that the intrinsic curvature and inter-wall interaction can induce a decrease of persistent current and change the shape of the flux-dependent current. A paramagnetism–diamagnetism transition is observed. With consideration of Zeeman splitting energy, the period of persistent current is destroyed. In addition, the effect of temperature and external electric field energy on persistent current is also explored. In the presence of external electric field, the persistent currents vary unmonotonously with $E_{\rm ef}$, and many isolated peaks of $I_{\rm ty}$ are obtained in a DWTCN at high electric field. By changing the value of $E_{\rm ef}$, a paramagnetism–diamagnetism or diamagnetism–paramagnetism transition is observed. These results can be helpful for our understanding of magnetic properties and potential applications of MWTCN devices.

References

[1] Liu J, Dai H, Hafner J H, Colbert D T, Smalley R E, Tans S J and Dekker C 1997 *Nature* **385** 780

[2] Matel R, Shea H R and Avouris P 1999 *Nature* **398** 299

[3] Sano M, Kamino A, Okamura J and Shinkai S 2001 *Science* **293** 1299

[4] Shea H R, Martel R and Avouris Ph 2000 *Phys. Rev. Lett.* **84** 4441
[5] Watanabe H, Manabe C, Shigematsu T and Shimizu M 2001 *Appl. Phys. Lett.* **78** 2928
[6] Lin M F, Chen R B and Shyu F L 1998 *Solid State Commun.* **107** 227
[7] Oh D-H, Park J M and Kim K S 2000 *Phys. Rev.* B **62** 1600
[8] Latgé A, Rocha C G, Wanderley L A, Pacheco M, Orellana P and Barticevic Z 2003 *Phys. Rev.* B **67** 155413
[9] Zhang Z H, Yang Z Q, Wang X, Yuan J H, Zhang H, Qiu M and Peng J C 2005 *J. Phys. Condens. Matter* **17** 4111
[10] Liu C P and Ding J W 2006 *J. Phys. Condens. Matter* **18** 4077
[11] Lin M F and Chuu D S 1998 *Phys. Rev.* B **57** 6731
[12] Liu L, Guo G Y, Jayanthi C S and Wu S Y 2002 *Phys. Rev. Lett.* **88** 217206
[13] Latil S, Roche S and Rubio A 2003 *Phys. Rev.* B **67** 165420
[14] Tsai C C, Shyu F L, Chiu C W, Chang C P, Chen R B and Lin M F 2004 *Phys. Rev.* B **70** 075411
[15] Tamura R, Ikuta M, Hirahara T and Tsukada M 2005 *Phys. Rev.* B **71** 045418
[16] Zhang Z H, Yuan J H, Qiu M, Peng J C and Xiao F L 2006 *J. Appl. Phys.* **99** 104311
[17] Lin M F 1999 *Physica* B **269** 43
[18] Liu C P, Ding J W and Chen H B 2008 *J. Phys. Condens. Matter* **20** 015206
[19] Lin M F 1998 *J. Phys. Soc. Jpn.* **62** 2218
[20] Lin M F 1998 *Phys. Rev.* B **58** 3629
[21] Shyu F L 2005 *Phys. Rev.* B **72** 045424
[22] Watanabe H, Manabe C, Shigematsu T and Shimizu M 2001 *Appl. Phys. Lett.* **78** 2928
[23] Cuniberti G, Yi J and Porto M 2002 *Appl. Phys. Lett.* **81** 850
[24] Chou Y Y, Guo G Y, Liu L, Jayanthi C S and Wu S Y 2004 *J. Appl. Phys.* **96** 2249
[25] Liu C P, Guo Z X, Ding J W and Yan X H 2005 *Physica* B **365** 109
[26] Colomer J F, Henrard L, Flahaut E, Tendeloo G V, Lucas A A and Lambin P 2003 *Nano Lett.* **3** 685
[27] Yu H, Zhang Q F, Luo G H and Wei F 2006 *Appl. Phys. Lett.* **89** 223106
[28] Froyen S and Harrison W A 1979 *Phys. Rev.* B **20** 2420
[29] Charlier J C, Lambin P and Ebbesen T W 1996 *Phys. Rev.* B **54** R8377
[30] Chen H B, Xu N and Ding J W 2008 *Solid State Commun.* **146** 12
[31] Xu N, Ding J W, Chen H B and Ma M M 2009 *Europ. Phys. J.* B **67** 71
[32] Rocha C G, Pacheco M, Barticevic Z and Latgé A 2004 *Phys. Rev.* B **70** 233402
[33] Xu N, Ding J W and Xing D Y 2008 *J. Appl. Phys.* **103** 083710
[34] Xu N, Ding J W, Chen H B and Ma M M 2009 *Chin. Phys.* B **18** 1674
[35] Xu N, Ding J W, Chen H B and Ma M M 2009 *Chin. Phys. Lett.* **26** 076107
[36] Liu C P and Xu N 2008 *Physica* B **403** 2884